

Dynamic Graph Streaming Algorithm for Digital Contact Tracing

Gautam Mahapatra, Priodyuti Pradhan, Ranjan Chattaraj and Soumya Banerjee

Abstract—Digital contact tracing of an infected person, testing the possible infection for the contacted persons, and isolation play a crucial role in alleviating the outbreak. Here, we design a dynamic graph streaming algorithm that can trace the contacts under the control of the Public Health Authorities (PHA). The algorithm can work as the augmented part of the PHA for the crisis period. Our algorithm receives proximity data from the mobile devices as contact data streams and uses a sliding window model to construct a dynamic contact graph sketch. Prominently, we introduce the edge label of the contact graph as a contact vector, which acts like a sliding window and holds the latest D days of social interactions. Importantly, the algorithm prepares the direct and indirect (multilevel) contact list from the contact graph sketch for a given set of infected persons. The algorithm also uses a disjoint set data structure to construct the infectious trees for the trace list. The present study offers the design of algorithms with underlying data structures for digital contact trace relevant to the proximity data produced by Bluetooth enabled mobile devices. Our analysis reveals that for COVID-19 close contact parameters, the storage space requires maintaining the contact graph of ten million users having 14 days close contact data in PHA server takes 55 Gigabytes of memory and preparation of the contact list for a given set of the infected person depends on the size of the infected list.

Index Terms—Contact graph, streaming algorithm, sliding window model, Bluetooth, disjoint set, COVID-19.

1 INTRODUCTION

Delaying in the vaccine or drug design increases the rapid spread of the COVID-19 disease. The current COVID-19 pandemic is caused by the droplet-based human to human transmission of SARS-CoV-2 [1]. At present, the whole human society is anxiously waiting for a possible new normal state of living. Almost every country adopts the social distancing along with lockdown to mitigate the pandemic [2]. Although complete lockdown reduces the risk of spread, extending the lockdown creates severe problems for the economy and the social life of the countries [3]. Also, as the pandemic stays a long time in a country, it becomes challenging to maintain the lockdown. Many countries ease the lockdown in terms of alternating and intermittent lockdown strategies to balance between

infection spread and economy [3], [4]. In this scenario, smartphone-based digital contact tracing becomes a promising approach to control the pandemic [1], [5], [6]. A recent study shows that highly effective contact tracing and case isolation is a good strategy to control a new outbreak of COVID-19 [7].

Contact tracing was a common and successful step to control several infectious diseases (e.g., Zika, HIV, influenza, Ebola viruses) [8], [9]. The World Health Organisation (WHO) defines contact tracing as the identification and follow-up of persons who may contact an infected person [8]. For COVID-19, two persons are in close contact if they are exposed to each other for at least fifteen minutes within one meter of distance [8]. The goal of contact tracing is to reduce a diseases effective reproductive number (R_0) by identifying people who have been exposed to the virus through the said close contact with an infected person and listing them for immediate quarantine or isolation. It has been reported that 46% contribution to R_0 comes from the presymptomatic individual (before showing symptoms) for COVID-19 [10]. On the other hand, COVID-19 infection is mostly asymptomatic nature. Hence, highly effective direct and indirect contact tracing is a mandatory task and plays a crucial role in early infection detection and reduces the peak burden on the healthcare system. Due to higher uncertainties in social relations, manual contact tracing to find the contact

- *Gautam Mahapatra is associated with Department of Computer Science, Asutosh College, University of Calcutta, Kolkata, West Bengal, India and Department of Computer Science and Engineering, Birla Institute of Technology, Mesra, Off-Campus Deoghar, Jharkhand, India. E-mail: gsp2ster@gmail.com*
- *Priodyuti Pradhan is associated with Complex Network Dynamics Lab, Department of Mathematics, Bar-Ilan University, Ramat-Gan, Israel. E-mail: priodyutipradhan@gmail.com*
- *Ranjan Chattaraj is associated with Department of Mathematics, Birla Institute of Technology, Mesra, Off-Campus Deoghar, Jharkhand, India. E-mail: chattaraj6@gmail.com*
- *Soumya Banerjee is associated with Inria EVA, Paris, France & Director Innovation Smart City EU. E-mail: dr.soumyabanerjee@ieee.org*

structure is a very complicated task for the PHA [11]. Recently, digital contact tracing uses low power radio frequency-based Bluetooth enabled mobile devices to overcome the problems in manual contact tracing. The success of TraceTogether of Singapore Government [12], COVID-Watch of Stanford University [13], [14], PACT of MIT [15], Exposure Notification forthcoming App of Apple-Google [16], Arogya Setu of MoHFA, Government of India [17] are all recent developments based on the Bluetooth technology to prepare the contact list more effectively to mitigate the COVID-19 pandemic [10], [18], [19], [20], [21], [22].

Although digital contact tracing substantially reduces human efforts, most smartphone apps store data locally in the device memory to maintain privacy [9]. Hence, the central authority has no control over the contact data. After detecting an infected person, PHA requests the person to donate the app data to make the trace list. As we know, a country's public health infrastructure is a national asset for which the government is responsible, and no pandemic can be addressed without a functional health system of the country [23]. Hence, to automate the trace list preparation in a regular interval, all proximity data should be automatically fetched by the PHA server from the registered devices and immediately stores in the form of ready to process structure. However, in the pandemic period, the vital question is how does the centralized control system store a large number of devices data as well as prepare direct and indirect contact lists about which little is known and remains elusive [24].

In this article, we provide a one-pass dynamic graph streaming algorithm with a sophisticated data structure to automate the multi-level digital contact tracing more accurately and efficiently of having centralized control under the PHA. After receiving the proximity data stream from the mobile devices, the algorithm uses a sliding window model to process the proximity data and dynamically evolves a close contact graph sketch. The nodes in the close contact graph are the individual users, and an edge is included if there exists an interaction between a pair of peoples for more than τ minutes within d meters distance in D days. Importantly, we introduce an edge label (interactions) between a pair of the individual in the contact graph as a fixed-sized binary first-in-first-out (FIFO) contact vector to reflect the communications in the last D days. In other words, during a pandemic, the contact graph stores the latest D days of continuous close contact data in a discrete form inside contact vectors. Finally, the system prepares the contact list for the given infected persons from the contact graph. We wish to emphasize that our algorithm prepares the direct and indirect (multi-level) contact list of the infected persons and stores in disjoint sets. We use the index file structure to store the large contact graph for

fast accessing. The salient feature of the system is that it automatically removes the inactive edge when the D days over and updates the graph through a sliding window model over the contact vectors. We provide implementation details and analysis of our devised streaming algorithm. Remarkably, our analysis reveals that for COVID-19 contact trace parameters, to store the contact graph for 14 days for 10^7 users take 55 GB of memory space. In addition, the preparation of the contact list for a given set of infected persons depends on the size of the infected list. Our algorithm is simple and easy to implement, and we expect it to be an attractive choice to deploy in the application of digital contact traces in real-world pandemic situations.

We fabricate the article as follows: Section 2 discusses the problem formulation and methodology of digital contact tracing process, Section 3 provide implementation detail of our dynamic graph streaming algorithm with sliding window model. Section 4 contains the space complexity of the contact graph and analyzes the contact trace algorithm. Finally, section 5 summarizes our work and discusses various open problems for further investigations.

2 METHODOLOGY AND RESULTS

At any time for infectious disease, we can divide the whole population (Σ) under a PHA jurisdiction into two disjoint sub-populations denoted as \mathcal{H} and \mathcal{I} . Here, \mathcal{H} and \mathcal{I} ($\mathcal{H} \cap \mathcal{I} = \emptyset$) represent healthy and infected subpopulations, respectively. Due to the contagious nature of the disease and human nature for social interactions, an infection may transmit from \mathcal{I} to \mathcal{H} and to stop the virus transmission chains, contact tracing became a non-pharmaceutical intervention to mitigate the outbreak [18]. Formally, a *close contact trace* for an infectious disease is a non-commutative binary operator, $\sigma_{(d,\tau,D)}$ between two individuals (P and P'), represented as $P\sigma_{(d,\tau,D)}P'$. This operator returns TRUE when a healthy person $P' \in \mathcal{H}$ has come in social contact with an infected person $P \in \mathcal{I}$ within d distance and remain exposed for at least τ min during infectious period D day so that infection may transmit from P to P' where τ , d and D are the close contact trace parameters. Using the operator, \mathcal{H} sub-divided into two sets where Γ and $\Delta (= \mathcal{H} - \Gamma)$. Here, Γ represents a set of uninfected (or suspected) persons who have been identified that they have come in close contact with an infected person(s) in \mathcal{I} during D days and it is the output of the close contact trace. On the other hand, Δ is the set of people who have not come in close contacts of any person in \mathcal{I} ; thus, they are free from infection. Therefore, repeated application of $\sigma_{(d,\tau,D)}$ on the members of \mathcal{I} and \mathcal{H} , we get contact tracing list, Γ . Monitoring proximity data of Bluetooth enabled digital communication devices; we

successfully design and implement the digital form of the close contact trace operator to generate a contact trace list.

2.1 Digitization of Close Contacts

A *close contact* between a pair of persons P and P' satisfies the maximum proximity distance d , minimum time duration within the proximity as τ min and at least one such event of closeness within D days of an infectious period so that infection may transmit between contacted persons [25]. Therefore, at any point in the immediate past of $24 \times 60 \times D = 1440D$ minutes after having an infection, the person can transmit the infection to another person who comes in the *close contact*. Hence, there is a maximum of $n = \lceil \frac{1440D}{\tau} \rceil$ number of non-overlapped consecutive time slots of spreading infections by an infected person. For instance, in COVID-19 pandemic, d is one meter, τ is 15 minutes, and to ensure close contact, we should hold $D = 14$ days data. To identify close contact, we subdivide the 14 days into 15 minutes time slots (i.e., n) and store one bit if there is a proximity contact in a particular time slot. In other words, our system converts continuous sensor data into the discrete close contact slots in the server data structure. Moreover, to improve the accuracy of proximity data acquisition by Bluetooth devices for the detection of close contact, we assume that 15 min time slot is further subdivided or sampled in 3 min (δ) time interval (i.e., D days contains $n' = \lceil \frac{1440D}{\delta} \rceil$ number of sample intervals where $\tau = \delta \times \rho$, ρ is a nonzero positive integer.

Here, we introduce a digitized form of *close contacts* between P and P' over the D days time window and represent as binary FIFO vector, denoted as $c = (c_{n-1}, \dots, c_1, c_0)$ where c'_i 's are different consecutive time slots, c_0 is latest, and c_{n-1} is the earliest (Fig. 1). Hence, any communication between a pair of persons is represented as a binary vector where each time slot stores one bit corresponding to τ min of time. Our system searches for contacts using proximity-based digital data communication performed by the mobile devices, which converts social asynchronous and analog contacts into the digital form. For this, employed smartphones sample the social contacts in δ time interval to collect data regarding the presence of a person within d distance. Now sampled digital data stream is analyzed through an watch window of length $\rho = \lceil \frac{\tau}{\delta} \rceil$ to identify close contacts. Our system continuously gets digital contacts and is recorded in contact vector c , which holds all close contact information between two individuals during the latest D days. Here, c helps to implement a digital form of $\sigma_{(d,\tau,D)}$, and with this, our system is transforming populations' close contact dynamics for the latest infectious period D into a ready to use dynamic contact graph sketch. Finally, for a given infected sub-population $\mathcal{I} \subseteq \Sigma$, our

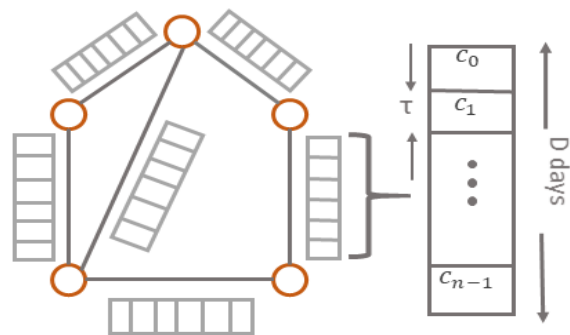


Fig. 1. Schematic representation of close contact graph (\mathcal{G}). We introduce edge label of \mathcal{G} as binary vector (c). Here, D is the observation period, τ is the time slot for exposure. For COVID-19, $D = 14$ and $\tau = 15$ minutes. We set c_k to be 1, when a close contact is detected at the k^{th} time slot duration and 0 otherwise.

algorithm uses $\sigma_{(d,\tau,D)}$ to prepare Γ from this contact graph sketch.

2.2 Contact Graph

We represent contact graph as $\mathcal{G} = \{V, E\}$ where $V = \{v_1, v_2, \dots, v_n\}$ is the set of vertices (nodes), represents members and $E = \{e_1, e_2, \dots, e_m | e_p = (v_i, v_j), p = 1, 2, \dots, m\}$ is the set of edges which are used to maintain the contact relation between members. For \mathcal{G} , edge relation encodes transmission of virus or infection from one person to other. Here, $V \equiv \Sigma$, so any P, P' and $P'' \in \Sigma$ are three individuals which are three different vertices in \mathcal{G} . When contact vectors between (P, P') and (P', P'') are non-zero ($c_{(P,P')} \neq \mathbf{0}, c_{(P',P'')} \neq \mathbf{0}$), then these are two different edges in \mathcal{G} . Note that these non-zero digital contact vectors help to implement $\sigma_{(d,\tau,D)}$ for \mathcal{G} . Now, if $P' \in \mathcal{I}$ then $P' \sigma_{(d,\tau,D)} P$ and $P' \sigma_{(d,\tau,D)} P''$ return TRUE, hence, P and P'' are included in Γ . However, if $P \in \mathcal{I}$ then $P \sigma_{(d,\tau,D)} P'$ returns TRUE, but $P' \sigma_{(d,\tau,D)} P''$ may not be TRUE due to the order of close contacts. We wish to emphasize that $\sigma_{(d,\tau,D)}$ returns FALSE when all close contacts between P' and P'' occur earlier than close contact(s) of P and P' . Therefore, $\sigma_{(d,\tau,D)}$ is not transitive. An operator is transitive means if P is related to P' and P' is related to P'' then it implies that P is also related to P'' [26]. Binary number representations of contact vectors play an crucial role in decision making of transitivity of $\sigma_{(d,\tau,D)}$. Hence, we need to store contact vectors to prepare the indirect or multi-level contact tracing list.

It has been reported that due to social relationships for a sufficiently large population, everyone is not coming in close contact with every other [30]. That means the average number of close contact relationships q is small compared to N ($q \ll N$), and hence \mathcal{G} is highly sparse. On the other hand, forming a close

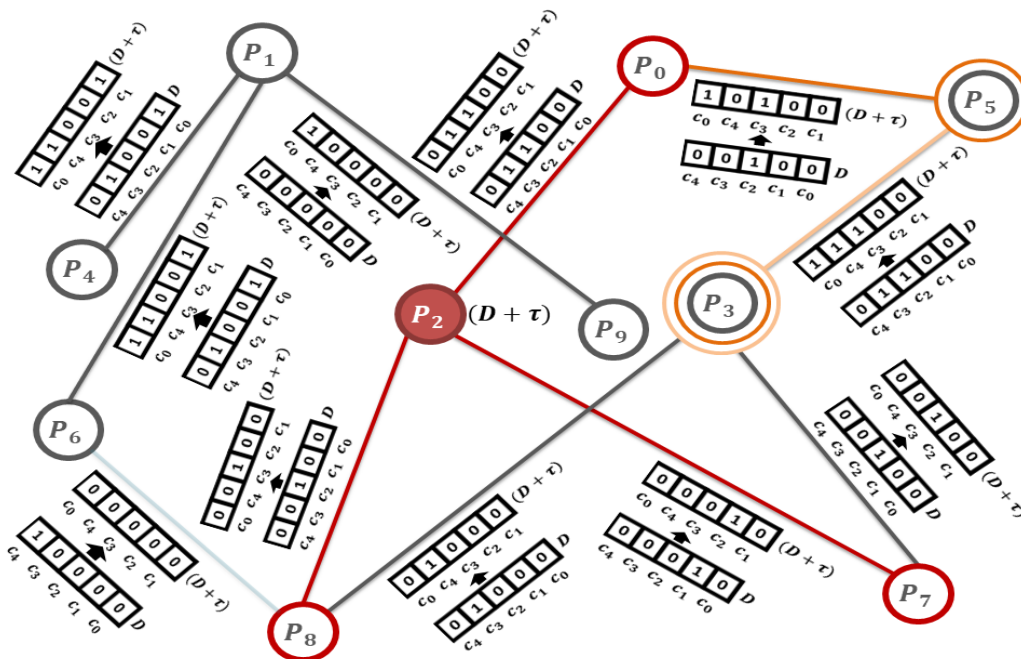


Fig. 2. Contact graph (\mathcal{G}) annotated with the contact vectors (c) at D and $D + \tau$ time instance. Here, we consider $N = 10$ and size of c is $n = 5$. One can observe that during the D days window, there is no close contact between P_1 and P_3 . However, as time progress the data streams from the devices at $D + \tau$, there is close contact between P_1 and P_3 ; thus, the algorithm sets one bit in $c_{(P_1, P_3)}$. Similarly, there is an edge between P_6 and P_8 during the D days window; however, at $D + \tau$ time slot, they have no close contact; thus algorithm removes this edge and updates \mathcal{G} . Further, for a given infected member P_2 , from \mathcal{G} by analyzing associated contact vector we get first-level contact list as $\{P_0, P_7, P_8\}$, second-level as $\{P_5\}$, and third-level as $\{P_3\}$ respectively.

contact requires human mobility, and coming close to each other, which is dynamic in nature. To store such sparse connectivity and the dynamic nature of human behavior, we use adjacency lists [26] and the respective digital contact vector to represent \mathcal{G} under the PHA server. Here, we use index-based [27] dynamic adjacency lists to maintain this fast access of ready-to-use digital form of \mathcal{G} so that direct contacts fetching for the generation of multi-level contact list becomes easy and accurate.

2.3 Contact Tracing

Here, we illustrate the contact tracing process with an example. Fig. 2 is a scenario of \mathcal{G} with ten individuals $\mathcal{H} = \Sigma = \{P_0, P_1, \dots, P_9\}$ with $n = 5$. Let us assume $\mathcal{I} = \emptyset$, $\Gamma = \emptyset$ at latest D^{th} day time instance. In our system, we can think \mathcal{G} which is a graph-based sliding watch window of digital close contacts. Here, \mathcal{G} is sliding one slot from D days i.e., from n^{th} slot instance to $(n + 1)^{\text{th}}$ slot. As D days infectious period is over so it shows the quitting of earliest slot and entering of latest slot using circular queue behaviour. Here, latest c_0 is assigned to the out going c_4 and earlier c_3 is now assigned to c_4 and so on, forming the one place logical shift (Appendix Fig. A1).

Now, let us assume that none is infected within the last D days duration (Fig. 2). However, at $D + \tau$ instance P_2 is detected as infected person (marked as red in Fig. 2) and immediately contact tracing is required. We can observe that P_0 , P_7 and P_8 are in direct close contact of P_2 in latest D days window, and will be in the adjacency list of P_2 . Hence, $\Gamma = \{P_0.1, P_7.1, P_8.1\}$ is the first-level (direct) close contact list of P_2 . To prepare the second-level (indirect) close contact list of P_2 , we observe that P_3 and P_5 are possible candidates (Fig. 2). However, we can not confirm this by observing only the edges. Now, we need to analyze the respective contact vectors to check the transitivity of $\sigma_{(d, \tau, D)}$. From the contact vectors one can observe that P_3 meets both P_7 and P_8 earlier than they are being exposed to virus transmission from P_2 , and there is no further close contact, therefore, P_3 will be excluded from Γ (Fig. 2). Whereas, P_5 has met with P_0 after the exposure of a virus of P_2 , so P_5 is coming into transitive closure relation of $\sigma_{(d, \tau, D)}$ and included in second-level contact. Moreover, during the latest D days window, P_3 comes in contact with P_5 , who may get a virus of P_2 and by extending the transitivity of $\sigma_{(d, \tau, D)}$, we can observe that P_3 will be included in the third-level contact list (Fig. 2). No further processing is possible and trac-

ing stops with $\Gamma(P_2) = \{P_0.1, P_7.1, P_8.1, P_5.2, P_3.3\}$, $\mathcal{I} = \{P_2\}$, $\Delta = \{P_1, P_4, P_6, P_9\}$ and $\chi = \{(P_2, P_8), (P_2, P_7), (P_2, P_0), (P_0, P_5), (P_5, P_3)\}$ where (P_i, P_j) represents P_i transmits infection to P_j .

Remarkably, the listing and pruning of second and higher-level contact list using $\sigma_{(d,\tau,D)}$ can be prepared through numerical operations on the equivalent decimal integer values of contact vectors. For any binary integer number, weight of higher significant position (2^i) is always greater than sum of all weights at lower significant positions ($i - 1$ to 0) [26]. For this reason, if the decimal value of any binary number (v_1) is greater than decimal value of another non-zero binary number (v_2), indicates that at least one close contact appears earlier for the close contact vector corresponds to v_1 than all close contacts corresponds to v_2 . From Fig. 2, the decimal integer values of $c_{(P_3,P_0)}$ and $c_{(P_0,P_5)}$ at $D + \tau$ time are $v_1 = c_4c_3c_2c_1c_0 = 11000 = 24$ and $v_2 = c_4c_3c_2c_1c_0 = 01001 = 9$ respectively. Here, $v_2 < v_1$ says at least one contact between P_2 and P_0 happened earlier than the contact between P_0 and P_5 . Hence, P_5 may get infection from P_0 as he/she has been exposed to the infected person P_2 and thus P_5 will be included in the second level contact list. Similarly, in case of P_3 , the c values with P_8 and P_7 (respectively 16 and 8) are greater in both cases than c values of P_8 and P_7 with the infected person P_2 (respectively 8 and 4). Hence, direct inclusion of P_3 into second level contact list is not required. Further, for i^{th} bit position of a binary number the weight is 2^i , i.e., power of two, so if any decimal value of c is power of two means only one close contact during D days, hence, analysis of other lower bit positions are not required for the confirmation of non-inclusion of P_3 . The value of $c_{(P_5,P_3)}$ is 25 which is greater than value of $c_{(P_0,P_5)}$ i.e., 9, but these are not power of two, so analysis of lower bit positions include P_3 as third-level member of the contact list. In this way, algorithm can implement $\sigma_{(d,\tau,D)}$ operator and use it to prepare the indirect contact list easily and accurately from \mathcal{G} .

3 IMPLEMENTATIONS

A particular jurisdiction has one PHA server that maintains all processing of the automated contact tracing process. We consider PHA employs Bluetooth enabled smartphones as the representatives of individuals for the automated data acquisition to implement the digital close contact trace operator ($\sigma_{(d,\tau,D)}$). Let T is the start time or deployment time of our system (in $dd/mm/yyyy : HH/MM$ format). On initialization, the PHA server creates an empty \mathcal{G} along with $\mathcal{I} = \emptyset$, $\mathcal{H} = \Sigma$ and hence $\Gamma = \emptyset$ and having population $\Sigma = \{P_0, P_1, \dots, P_{N-1}\}$. Here, the population is identified by the first N positive integers starting from zero. Now, to maintain privacy during Bluetooth

communication, it is not possible to know the assigned phone number of a nearby person comes into social contacts [12]. Hence, Bluetooth-based short-distance broadcasting uses virtual IDs. After deployment, in a regular interval, the PHA server randomly generates a set of virtual IDs for whole populations Σ . For this purpose, non-negative natural numbers (\mathbb{N}) are sub-divided into N numbers of non-overlapping sets each of size $r (\geq 1)$, i.e., $\pi = \{\pi_1, \pi_2, \dots, \pi_N\}$, where $\pi_i = \{k_1, k_2, \dots, k_r\}$, $\pi_i \cap \pi_j = \emptyset$, $|\pi_i| = r$, $k_i \in \mathbb{N}$. Now server randomly assigns π_i to the different members in Σ . Now, the system is ready to receive contact data streams from mobile devices under PHA, and evolving of \mathcal{G} begins. Consider P and P' are two distinct Bluetooth enabled smartphones. Let $\pi_P \equiv \pi_i$ and $\pi_{P'} \equiv \pi_j$ assigned virtual IDs sets for P and P' respectively. Next, P and P' randomly choose $k_i \in \pi_P$ and $k_j \in \pi_{P'}$ and used as virtual IDs. Now, when both P and P' (or others) come in social contact with a minimum distance (d) confirmed by the Bluetooth signals, respective devices broadcast messages using their virtual IDs in δ time intervals [28]. During this communication, P receives messages from P' with used virtual ID and vice-versa. These transmitted and received messages are locally stored in the device memory, and the send/receive time-stamp. As both P and P' are having multiple assigned IDs, in a specific time period, they use separate k_i and k_j as their virtual IDs. Finally, devices pre-process the proximity data locally and send as data stream represented as Ω to the PHA server to identify the close contact(s). In the following sections, we provide an implementation detail of \mathcal{G} .

3.1 Data Structure for Contact Graph Sketch

We represent \mathcal{G} using adjacency lists having two components, index file ($\mathcal{G}.\Psi$) and contact record or data file ($\mathcal{G}.\Theta$). The $\mathcal{G}.\Psi$ stores q number of index records with two fields ($UserID, Pointer$) for each user (Fig. 3). Here, q , the average degree of the \mathcal{G} represents the average number of distinct persons coming in close contacts to a person during D days. Moreover, we maintain one extra index record in $\mathcal{G}.\Psi$ to move into the overflow area when contacts exceed the average value of q .

For each pairs of individuals, we store c only once in $\mathcal{G}.\Theta$ at A index position. For an edge $e = (P, P', c_{(P,P')})$, P' will appear as one record (P', A) under P . Similarly, we keep another record (P, A) under P' . For an implementation, D and τ are fixed implies size of c is also fixed. Also, we assume in an average there are q number of distinct close contacts during D days period. Therefore, we can access both $\mathcal{G}.\Psi$ and $\mathcal{G}.\Theta$ as an array with constant access time. Here, algorithm uses $\mathcal{G}.\Psi[P(q+1)]$ to access the starting contact record of P . Similarly, $\mathcal{G}.\Theta[(A) \times n]$ uses

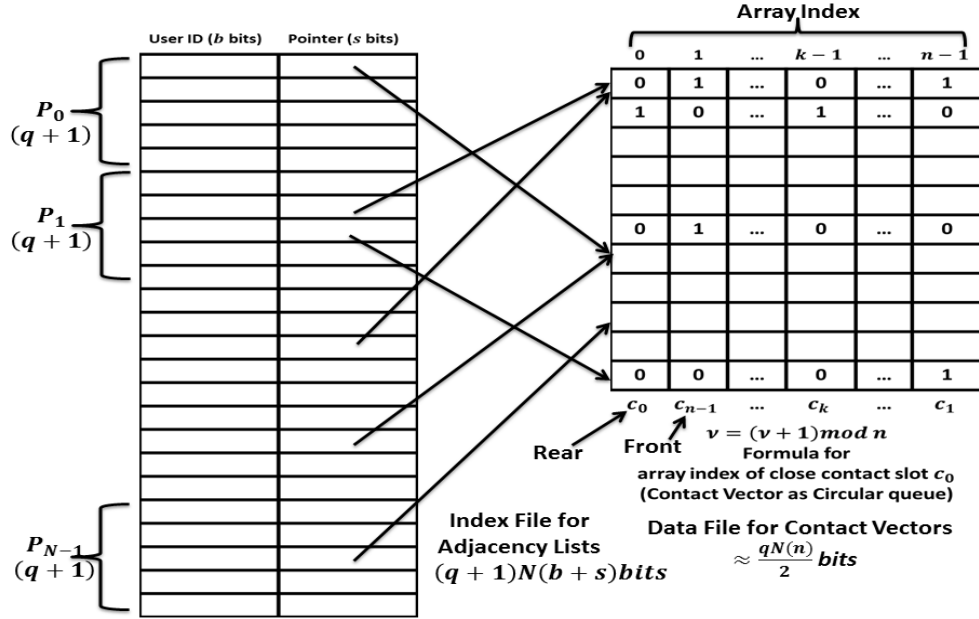


Fig. 3. Data Structure for the contact graph (\mathcal{G}). Here, $\mathcal{G}.\Psi$ is the index representation of adjacency lists of N persons as (*UserID*, *Pointer*). The $\mathcal{G}.\Theta$ holds fixed size contact vectors c of size n . Both are in the form of array. Here, $(q+1)^{th}$ index record for each user is assigned to enter into the respective overflow area.

to access the first bit of c . In addition, to access the overflow area we use $\mathcal{G}.\Psi[P(2q+1)]$ [29]. Therefore, \mathcal{G} can watch every close contact of the society for latest D days and reflecting as sliding watch window with all c_0 is the close contact front of the Σ .

3.2 Embedding data stream into contact graph

The PHA server receives the contact data stream (Ω) from registered mobile devices (Fig. 4). The Ω contains a header part and communication details. The header part holds actual sender ID as P in $\Omega.UID$ and broadcast start time as $\Omega.StartTime$ as t . Further, communication details contain $\Omega.Tran$ and $\Omega.Rec$ for transmitted and all received virtual user IDs during proximity contact (Fig. 4). Note that mobile devices sample for the proximity of neighbors in δ time intervals and send processed contact information in the form of a data stream to the PHA server (Fig. 4). A valid close contact requires τ min of continuous proximity neighbors' data. Here, we consider $\tau = \delta \times \rho$ min, i.e., if someone is present nearby with a person for a continuous ρ number of samples, then there will be a close contact. Hence, to detect close contact during stream processing, the algorithm uses a sliding window (\mathbf{W}) of size ρ . For COVID-19, one can set $\delta = 3$ min, and thus, $\rho = 5$, and hence, to ensure a close contact, one person should appear 5 times inside \mathbf{W} . Therefore, to process stream data of mobile devices and detect close contact, we use one sliding

window. On the other hand, contact vector (c), which always holds the latest D days binary close contact data, is another sliding window. The first window is implemented as a FIFO queue, and the second one is implemented as a FIFO circular queue, and we always insert data at REAR and remove from FRONT of the queue. Hence, maintaining \mathcal{G} is the interplay between two sliding windows. Here, latest slot (c_0) of c always appears at REAR and earliest slot (c_{n-1}) at the FRONT of the queue and we can find c_0 at array index $\nu \leftarrow (\nu+1) \bmod n$. For circular behavior of modulo-arithmetic when queue becomes full after passing D days, c_0 returns to the $\nu = 0$ index location and c_{n-1} appears at array index 1 and so on (Fig. 3 and Appendix Fig. A1).

In Fig. 4, we show that at the beginning of interval of the proximity contact data for a new user ($P = P_2$), algorithm creates an empty \mathbf{W} . Now, PHA server determines the actual user IDs (e.g., P_1 for 4, P_3 for 8) from virtual user IDs (4 and 8) in $\Omega.Rec$ field of the current sample data and store temporarily inside $U(\{P_1, P_2\})$. Therefore, (P_2, P_1) and (P_2, P_3) are two proximity contacts in this current sample interval and stored at $\mathbf{W}[0]$ in a linked list form with associated communication count (ϱ) value set to one ($P_1.\varrho = P_3.\varrho = 1$). Similarly, for next interval data, we get same situation and the corresponding linked list is stored at $\mathbf{W}[1]$. However, to indicate the appearance of an user in \mathbf{W} , ϱ value of the earlier communication with

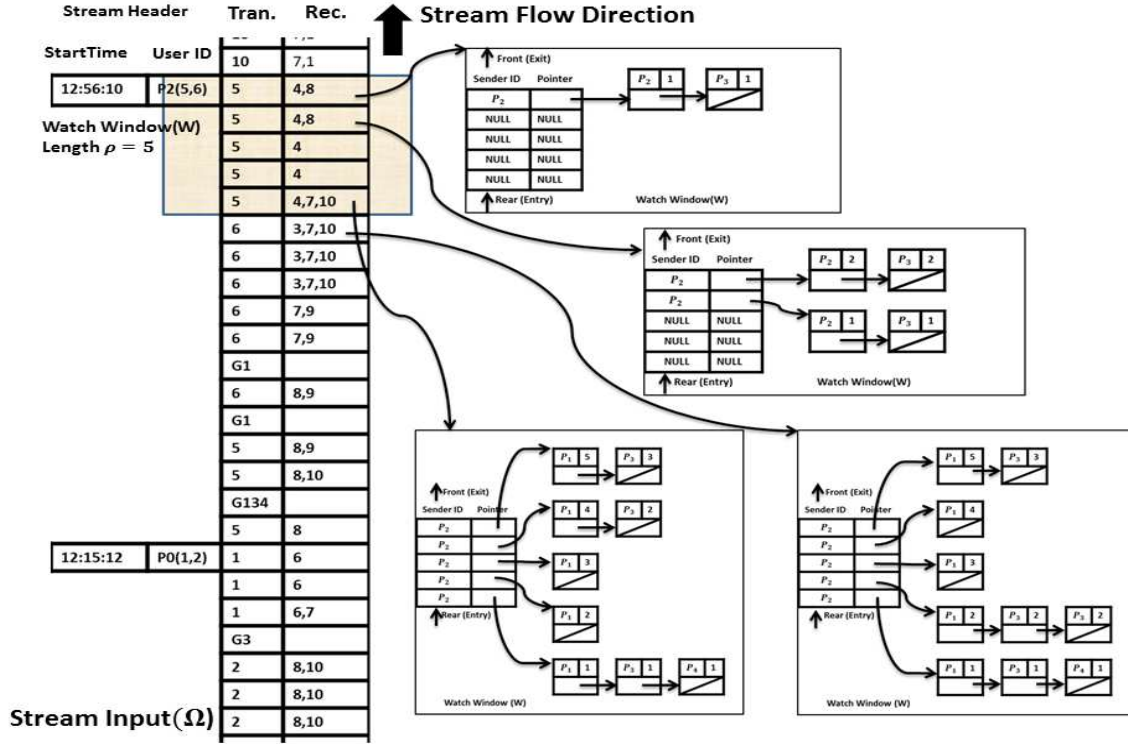


Fig. 4. Processing proximity data stream (Ω) and detect close contact through a watch window (\mathbf{W}). The PHA server assigns virtual IDs to the users P_0, P_1, \dots, P_{N-1} as $\pi_{P_0} = \{1, 2\}, \pi_{P_1} = \{3, 4\}, \dots, \pi_{P_{N-1}} = \{2N-1, 2N\}$. Individuals communicate with each other through virtual IDs during broadcast and appears in the *Tran.* and *Rec.* fields in Ω . For every user, Ω begins with a start time (t) and actual user ID of the sender. The \mathbf{W} is a fixed size ($\rho = 5$) array of pointers which works as a FIFO queue where data enters at the REAR and exits from FRONT. The window and holds proximity data for latest ρ intervals. Each entry of \mathbf{W} holds actual sender ID and the list of actual receiver IDs in a linked list form. Receiver ID in \mathbf{W} associates a communication count value (ϱ) to count the appearance in ρ number of intervals. During removal from FRONT of \mathbf{W} if the ϱ of any user P' is equal to ρ then it is a close contact between P and P' . A pointer field is NULL, means there is no proximity communication in the next interval.

persons in U are increased by one for record at $\mathbf{W}[0]$ ($P_1.\varrho = P_3.\varrho = 2$). Similarly, processing continues until \mathbf{W} is full. Now, to accommodate the next interval data at REAR, algorithm removes elements from FRONT at $\mathbf{W}[0]$. After removal, algorithm checks ϱ value for an user. If it is equal to ρ , then it is a close contact. Here, one can observe that for $P_1.\varrho = \rho$ (Fig. 4). Hence, P_1 was in proximity contact for latest all ρ number sample intervals leading to a close contact with P_2 . Therefore, we require to install into c_0 slot of the contact vector ($c_{(P_2, P_1)}$) in \mathcal{G} . However, (P_2, P_3) is not a close contact as $P_3.\varrho \neq \rho$.

Now, to embed the detected close contact in \mathcal{G} , we determine the array index number (ν) for c_0 of c by synchronizing the start time (t) of P with the system start time (T) (Eq. 1). Also, note that due to unpredictable nature of human communication, the close contact may appear at any time. That means first sample interval of close contact may be at any of ρ number of intervals in earlier slot i.e., c_1 and accordingly ends at any of ρ number of sample intervals in

c_0 slot (Fig. 5). In this situation, we select suitable one for c_0 and c_1 depending on the most proximity contact intervals (Fig. 5). Therefore, to make decision about c_0 and c_1 , we also synchronize t of P with T for the interval number (λ) of the current ν (Eq. 1).

$$\nu = \left\lfloor \frac{T'}{\tau} \right\rfloor \bmod n, \quad \lambda = \left\lfloor \frac{T'}{\delta} \right\rfloor \bmod n' \quad (1)$$

where $T' = (1440 \times X.Days + 60 \times X.Hrs + X.Min)$ and $X = T - t$ (date difference), here T is the system deployment time, both t and T are in format $dd/mm/yyyy : hh : mm$ and date difference $T - t$ is in format $Days/Hrs/Min$, and $n' = \lfloor \frac{1440D}{\delta} \rfloor$. Further, when there is no communication for one or more δ time interval(s) between nearby Bluetooth devices, we consider the next record in Ω is of Gx format, indicating that there is a communication gap for $x(\geq 1)$ number of δ time intervals. For Gx , we update ν and λ for starting slot (c_0) using Eq. (2) to skip x number

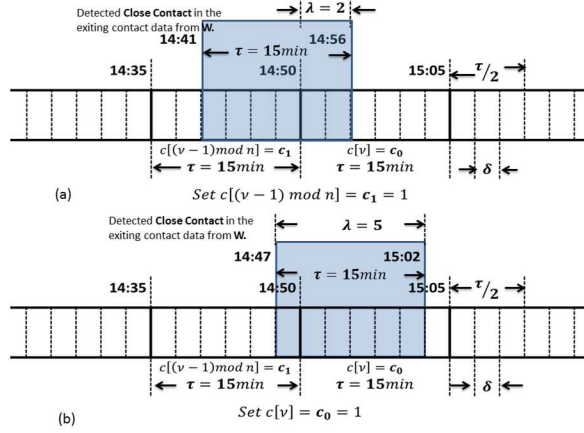


Fig. 5. Resolving the conflict between slot numbers (c_1 and c_0) of c for a detected close contact at c_0 . The maximum part of the close contact duration lies (a) in c_1 slot and (b) in c_0 slot.

intervals.

$$\nu = \left(\nu + \left\lfloor \frac{x}{\rho} \right\rfloor \right) \bmod n, \quad \lambda = (\lambda + x) \bmod \rho \quad (2)$$

Now, in Fig. 5, we show how ν and λ are used to identify correct slot in c accordingly update the detected close contact in \mathcal{G} . Here, $c[\nu]$ is equivalent to c_0 slot, and $c[(\nu - 1) \bmod n]$ is the immediate earlier slot c_1 . Now, we divide close contact duration $\tau = 15$ min into $\rho = 5$, number of sample intervals each of length $\delta = 3$ min. Here, half of the number of sample intervals is $\lfloor \frac{\rho}{2} \rfloor = 2$. In Fig. 5 (a), we show that current close contact watch window ends before half of the number intervals of c_0 slot ($\lambda = 2 \leq \lfloor \frac{\rho}{2} \rfloor$). This indicates that most of the part of current close contact exists in the immediate earlier slot, so $c_1 = 1$. Similarly, in Fig.5 (b), we show $\lambda = 5 (> \lfloor \frac{\rho}{2} \rfloor)$, that means most of part of current \mathbf{W} exists in the latest slot, so $c_0 = 1$. In this way conflict for c_1 and c_0 is resolved.

Finally, $Set()$ function is used to perform these changes of c in \mathcal{G} . The process will continue for the whole contact data stream of the different users (Algorithm 1). Algorithm 2 helps to install any detected close contact (P, P', ν, λ) into \mathcal{G} during data stream processing. To install the close contact for P , search starts from $\mathcal{G}.\Psi[P(q + 1)]$ location of the index file. If it is successful then update is performed in the target slot. However, on an unsuccessful search, the algorithm creates an empty contact vector in $\mathcal{G}.\Theta$ and accordingly updates the target slot. New contact vector means new relation between P and P' and hence, we also update $\mathcal{G}.\Psi$ (Algorithm 1). As time passes, the social contact dynamics are changing, and some contacts are older than infectious duration D . Hence, the

Algorithm 1 Process(\mathcal{G}, Ω)

```

while (Buffer( $\Omega$ )  $\neq$   $\phi$ ) do
  if ( $\Omega.StartTime \neq \phi$ ) then
     $t, P \leftarrow \Omega.StartTime, \Omega.UID$ 
     $\nu, \lambda, \rho, W \leftarrow Initialize(t)$ 
  end if
   $X \leftarrow GetNext(\Omega.Data)$ 
  if ( $X = Gx$ ) then
     $\nu, \lambda, W \leftarrow Update(\nu, \lambda, x)$ 
  else
     $U \leftarrow GetUsers(X.Rec, t)$ 
     $U.q \leftarrow 1$ 
     $W \leftarrow UpdateCounters(W, U)$ 
    if ( $Size(W) = \rho$ ) then
       $W \leftarrow Delete(W, U')$ 
      for all ( $P'$  in  $U'$ ) do
        if ( $P'.q = \rho$ ) then
           $\mathcal{G} \leftarrow Install(\mathcal{G}, P, P', \nu, \lambda)$ 
        end if
      end for
    end if
    if  $\lambda = \rho$  then
       $\nu \leftarrow (\nu + 1) \bmod n$ 
    end if
     $\lambda \leftarrow (\lambda + 1) \bmod \rho$ 
     $W \leftarrow Insert(W, U)$ 
  end if
end while
return  $\mathcal{G}$ 

```

edge(s) along with contact vector(s) will be removed from \mathcal{G} .

3.3 Contact Tracing on \mathcal{G}

The \mathcal{G} maintains the digital form of the social contact dynamics of Σ for the particular geopolitical area under a PHA for the last D days. We assume that at any time, the system has a contact trace list (Γ) for a given set of infected persons (\mathcal{I}), and the rest are uninfected individuals (Δ). Now, we iteratively update the contact list as follows.

Now, suppose at present, one or more individuals are detected as a newly infected person and kept in \mathcal{I}' . After receiving \mathcal{I}' , system will perform immediate contact tracing in \mathcal{G} where $\mathcal{I}', \Gamma, \mathcal{G}$ and L are passed as input parameters (Algorithm 3). Here, L means up to which level indirect contacts will be traced. The algorithm returns updated Γ , which contains first, second, and other required higher levels of indirect contacts along with respective edge list χ' . Finally, we update new infected list as $\mathcal{I} \leftarrow \mathcal{I} \cup \mathcal{I}'$, new uninfected list as $\Delta \leftarrow \Delta - \Gamma$ and new edge list as $\chi \leftarrow \chi \cup \chi'$. If a person appears more than one contact list, Algorithm 3 automatically remove the redundancy.

Algorithm 2 $\text{Install}(\mathcal{G}, P, P', \nu, \lambda)$

```

 $A \leftarrow \text{Search}(\mathcal{G}.\Psi, P, P')$ 
if ( $A \neq \text{NULL}$ ) then
   $A \leftarrow \mathcal{G}.\Psi[A].\text{Pointer}$ 
else
   $A, \mathcal{G}.\Theta \leftarrow \text{GetContactVector}(\mathcal{G}.\Theta)$ 
   $B_1, \mathcal{G}.\Psi \leftarrow \text{GetIndexRec}(\mathcal{G}.\Psi, P)$ 
   $B_2, \mathcal{G}.\Psi \leftarrow \text{GetIndexRec}(\mathcal{G}.\Psi, P')$ 
   $\mathcal{G}.\Psi[B_1].\text{UID} \leftarrow P'$ 
   $\mathcal{G}.\Psi[B_2].\text{UID} \leftarrow P$ 
   $\mathcal{G}.\Psi[B_1].\text{Pointer} \leftarrow A$ 
   $\mathcal{G}.\Psi[B_2].\text{Pointer} \leftarrow A$ 
end if
 $\mathcal{G}.\Theta \leftarrow \text{Set}(\mathcal{G}.\Theta[A], \nu, \lambda)$ 
return  $\mathcal{G}$ 

```

The algorithm uses two queues Q_1 and Q_2 alternatively as processing and waiting of individuals to trace close contact (Algorithm 3). Initially, we set current contact level number $l = 1$ (direct or first-level contact), and all members in \mathcal{I}' are in the processing queue (Q_1) and hence, Q_2 is empty and working as waiting queue. Now, for all members in the Q_1 direct contact list are generated from indexed adjacency list in $\mathcal{G}.\Psi$ and stored in Γ as well as in the waiting queue (Q_2). For higher-level contact tracing we update l , swap Q_1 and Q_2 and then use the transitivity of $\sigma_{(d,\tau,D)}$ (Algorithm 3).

In section 2.3, we explain the different such situations for filtering the second and higher-level contact tracing for which bit-patterns of c and decimal values are used to exclude or include next member in the contact list and also pruning of further processing. The process will continue either up to the state with no more individuals left in the waiting queue or target level (L) of indirect contacts has reached (Algorithm 3).

3.4 Disjoint Sets for Contact Trace Results

Practically the contact trace output divides the whole population into three different disjoint sub-populations - namely infected (\mathcal{I}), suspected (Γ), and uninfected (Δ). The system also generates the edge list (χ) of the suspected members (Algorithm 3). There are general questions from the perspective of management - how many clusters of infected groups list the members of these clusters, the order of spreading, or refer as infectious trees. Only Γ is not sufficient to meet these requirements, and we cannot answer only from Γ . We use Disjoint Set Data structure (DSD) denoted as \mathcal{F} to address the above queries [26]. Initially, Σ , \mathcal{F} maintains N number of rooted single node disjoint trees all marked with status 'Free' and $\mathcal{F}.\text{EdgeList}$ is empty. Rebuild algorithm of DSD use results from the contact

Algorithm 3 $\text{TraceContacts}(\mathcal{G}, \mathcal{I}', \Gamma, L)$

```

Create  $\chi, Q_1, Q_2, l$ 
for all  $P \in \mathcal{I}'$  do
   $A \leftarrow P(q + 1)$ 
  while  $\mathcal{G}.\Psi[A].\text{Pointer} \neq \text{NULL}$  do
     $P' \leftarrow \mathcal{G}.\Psi[A].\text{UID}$ 
    if  $P' \notin \Gamma$  then
       $P'.\text{Level} \leftarrow l$ 
       $\Gamma \leftarrow \Gamma \cup P'$ 
       $\chi \leftarrow \chi \cup \text{Edge}(P, P')$ 
       $Q_1 \leftarrow \text{Insert}(Q_1, A)$ 
    end if
     $A \leftarrow A + 1$ 
  end while
end for
 $l \leftarrow l + 1$ 
while ( $(l \leq L)$  and not ( $\text{IsEmpty}(Q_1)$  and  $\text{IsEmpty}(Q_2)$ )) do
  while (not  $\text{IsEmpty}(Q_1)$ ) do
     $Q_1 \leftarrow \text{Delete}(Q_1, A)$ 
     $P \leftarrow \mathcal{G}.\Psi[A].\text{UID}$ 
     $A' \leftarrow P(q + 1)$ 
    while  $\mathcal{G}.\Psi[A'].\text{Pointer} \neq \text{NULL}$  do
       $P' \leftarrow \mathcal{G}.\Psi[A'].\text{UID}$ 
      if  $P' \notin \Gamma$  and  $\text{Execute-}\sigma_{(d,\tau,D)}(A, A')$  then
         $P'.\text{Level} \leftarrow l$ 
         $\Gamma \leftarrow \Gamma \cup P'$ 
         $\chi \leftarrow \chi \cup \text{Edge}(P, P')$ 
         $Q_2 \leftarrow \text{Insert}(Q_2, A')$ 
         $A' \leftarrow A' + 1$ 
      end if
    end while
  end while
   $Q_1, Q_2 \leftrightarrow Q_2, Q_1$ 
end while
return  $\Gamma, \chi$ 

```

trace algorithm to update \mathcal{F} and $\mathcal{F}.\text{EdgeList}$ stores all edges in χ (Algorithm 4). Now, using *union - find()* operation of DSD, all edges in χ are processed to form the final disjoint sets. Nodes are also marked according to 'Infected' and 'Suspected'. For any individual, *find()* returns the tree's root, which means the group or cluster in which the individual is a member. Further, traversing this rooted tree provides the full cluster, size of the cluster, and the order of spreading or infectious tree. The number of such rooted trees in the \mathcal{F} is the count of the disjoint sets, i.e., the number of clusters exists presently in the PHA. Each such cluster is an infection zone with separate active infections and suspected members under the isolation process. In this way, if the contact tracing result is stored in a DSD structure, then taking different management decisions during a pandemic will be easy.

Algorithm 4 BuildDisjointSet($\mathcal{F}, \chi, \mathcal{I}, \Gamma$)

```

while ( $\chi \neq \phi$ ) do
   $\xi \leftarrow \text{RemoveNext}(\chi)$ 
   $A \leftarrow \text{Insert}(\mathcal{F}.\text{EdgeList}, \xi)$ 
   $i \leftarrow \text{Find}(\mathcal{F}, \xi.P)$ 
   $j \leftarrow \text{Find}(\mathcal{F}, \xi.P')$ 
  if  $i \neq j$  then
     $\mathcal{F} \leftarrow \text{Union}(\mathcal{F}, i, j, A)$ 
  end if
end while
return  $\mathcal{F}$ 

```

4 PERFORMANCE ANALYSIS

4.1 Space complexity analysis

Here, we calculate the space requirement to store the graph sketch for the D days proximity data of N number of users as adjacency list representation (Fig. 3). We know \mathcal{G} has two parts $\mathcal{G}.\Psi$ for index store and $\mathcal{G}.\Theta$ for data store and space requirement is denoted as $\mathcal{S}(\mathcal{G}.\Psi)$ and $\mathcal{S}(\mathcal{G}.\Theta)$ respectively. We need $b = \lceil \log_2 N \rceil$ bits to access ID of the N number of different users. Next, we assume in an average there are q number of distinct close contacts during a time period of D days or n ($n = \lceil \frac{1440D}{\tau} \rceil$) number time slots of duration τ min. For each user, we store $q + 1$ number of direct index records in $\mathcal{G}.\Psi$ and for these direct records $\frac{qN}{2}$ number contact vectors each of $(n + 1)$ bits (one extra bit for deletion flag) are stored in $\mathcal{G}.\Theta$. To identify each such contact vector, we require $s = \lceil \log_2 \frac{qN}{2} \rceil$ bits index in the pointer field of the index record. Therefore, the space requirement for $\mathcal{G}.\Psi$ is

$$\begin{aligned} \mathcal{S}(\mathcal{G}.\Psi) &= (q + 1)N(b + s) \\ &= (q + 1)N(2 \log N + \log q - 1) \\ &= \mathcal{O}(N \log N) \end{aligned}$$

bits. Similarly, for $\frac{qN}{2}$ number of records in $\mathcal{G}.\Theta$ is

$$\mathcal{S}(\mathcal{G}.\Theta) = \frac{qN}{2}(n + 1) = \mathcal{O}(N)$$

bits. Hence, the total space requirement (in bits) is

$$\begin{aligned} \mathcal{S}(\mathcal{G}) &= \mathcal{S}(\mathcal{G}.\Psi) + \mathcal{S}(\mathcal{G}.\Theta) \\ &= N \left[(q + 1)(2 \log N + \log q - 1) + (n + 1) \frac{q}{2} \right] \\ &= \mathcal{O}(N \log N) \end{aligned} \tag{3}$$

Study shows that for a very small percentage of cases overflow area is required [30]. Hence, the additional memory requirement will be nominal. Here, D , τ , and q are constant for a particular type of infection, and hence, we get the space complexity of \mathcal{G} is $\mathcal{O}(N \log N)$.

For COVID-19 outbreak, we assume for population of $N = 10^7$, the length of infectious period

$D = 14$ days, minimum time of contact $\tau = 15$ min at maximum separation of one meter. To estimate q , we use statistics from a recent UK based social contact survey [30]. It suggests that for COVID-19 pandemic the average number of contacts (q) over 14 days is 217. However, only 59 (27%) of contacts are meeting close contact definition [11], [30]. With this statistics, we choose $q = 64$. Hence, the estimated storage requirements for \mathcal{G} using Eq. (3) is:

$$\begin{aligned} \mathcal{S}(\mathcal{G}) &= 10^7 [(64 + 1)(2 \log 10^7 + \log 64 - 1) \\ &\quad + \left(\frac{1440 \times 14}{15} + 1 \right) \frac{64}{2}] \times 2^{-33} \text{ GB} \\ &\approx 55 \text{ GB as } 1 \text{ GB} = 2^{33} \text{ bits.} \end{aligned}$$

4.2 Time complexity

The system has three parts for the operation - (a) detecting and then storing of digital close contacts during stream processing, (b) tracing of multi-level contacts for a set of infected individuals and (c) storing tracing results in the disjoint set data structure to answer different standard management and control operations.

To detect a close contact in Ω and installation into \mathcal{G} , requires maximum q number array index manipulations. We assume q is constant and independent of N , thus average number of computation required for the processing of Ω is constant and hence, time complexity is $\mathcal{O}(1)$. The \mathcal{G} is a ready to use form for contact tracing. Computation complexity for the preparation of Γ has two parts - computation counts for direct list preparation denoted as $(T_{direct}(q, L, n, N))$ and for indirect list as $(T_{indirect}(q, L, n, N))$. Now, we evaluate $T_{direct}(q, L, n, N)$ for given \mathcal{I} as follows. For any infected person P in \mathcal{I} , we access at most q number of consecutive pointer field in $\mathcal{G}.\Psi$ array. We know that one can reach to the beginning of the adjacency list of P using $\mathcal{G}.\Psi[P(q + 1)]$ (section 3.1). Therefore, total pointer comparison count takes

$$T_{direct}(q, L, n, N) = q \times |\mathcal{I}| = \mathcal{O}(q|\mathcal{I}|) \tag{4}$$

However, to prepare the second level contact list, we perform n bits contact vector comparison to execute $\sigma_{(d, \tau, D)}$ for each members in the direct contact list of $q \times |\mathcal{I}|$ individuals (Algorithm 3) is $q \times (q \times |\mathcal{I}|)$, and for third-level it is $q \times (q^2 \times |\mathcal{I}|)$ and so on. Hence, the total computation complexity for indirect levels is

$$\begin{aligned} T_{indirect}(q, L, n, N) &= n[q \times (q \times |\mathcal{I}|) + q \times (q^2 \times |\mathcal{I}|) \\ &\quad + \dots + q \times (q^{L-1} \times |\mathcal{I}|)] \\ &= q^2 \times \frac{(q^{L-1} - 1)}{(q - 1)} \times (|\mathcal{I}| \times n) \\ &= \mathcal{O}(q^L |\mathcal{I}|) \end{aligned}$$

Now, for both direct and indirect contact list tracing computation takes

$$T(q, L, n, N) = \mathcal{O}(q^L |\mathcal{I}|)$$

Finally, for disjoint set representation having $|\Gamma|$ of contact trace members with $|\chi|$ number edges takes $\mathcal{O}(|\chi| \alpha(|\Gamma|))$ where $\alpha()$ is the *Inverse Ackermann()* function, $\alpha() \leq 5$ [26]. From the above analysis, we can show that for COVID-19 contact trace parameters, to prepare the contact list for a given \mathcal{I} , it takes $\mathcal{O}(|\mathcal{I}|)$ when q and L are constant.

5 CONCLUSION

In this article, we design a dynamic graph streaming algorithm with sophisticated data structures for a digital contact tracing system to mitigate the spreading of a contagious outbreak under the control of the Public Health Authority of a country. After receiving the data stream from the mobile devices, the algorithm uses a sliding window model to convert continuous proximity-based device data into the discrete close contact slots and convert it into a fixed-length bit pattern and stored in the contact vector. Finally, in the server, all close contact vectors use to form an efficient dynamic contact graph sketch. Once the server maintains the close contact graph sketch, our algorithm prepares the direct and indirect (multilevel) contact list of the infected persons and stores in disjoint sets. We use the index file structure to store the large contact graph in an array. Here, we use two sliding windows, one to process the stream data of mobile devices and detection of close contacts and another sliding window use to maintain the close contact vector over D days period. The first one is implemented as a FIFO queue, and the second one is implemented as a FIFO circular queue. Our framework is relevant to general contact-transmitted diseases like COVID-19 and can trace digital contact for other infectious diseases by changing the parameters of the contact trace operator. Heart of our algorithm is the contact trace operator, which uses numerical computation over the binary number stored inside the contact vector to decide the multilevel contact trace list. Our analysis unveils that for COVID-19 outbreak close contact parameters, the storage space requires maintaining the contact graph of 10^7 individuals having 14 days close contact data in PHA server takes 55 Gigabytes of memory and prepares the contact list for \mathcal{I} takes $\mathcal{O}(|\mathcal{I}|)$.

The binary representation of close contact is an integral part of our algorithm. Importantly, interactions between a pair of the individual are annotated as a binary circular vector to elucidate the communication in a different time and capture a complete picture of the social interactions. Therefore, dynamic contact graph sketch reflects the population dynamics of the

jurisdiction and can be used for further study related to epidemic dynamics to predict the trajectory of the spread accurately [18]. Here, we develop the algorithm relevant to the proximity data of Bluetooth enabled mobile devices. However, we can easily extend the algorithm for Global Positioning Systems (GPS) based sensor data with some modification and further research [19]. Although our goal is to provide space-efficient and an easily accessible digital contact tracing algorithm under the control of PHA and prepare the direct as well as indirect contact list, however, considering the virtual ID and binary contact vector, the algorithm implicitly enforces the privacy of users. For more details of the privacy concern of the digital contact trace, we refer to the current articles [17], [31], [32]. On the other hand, the sliding window model is space-efficient and can have a further application from the applied and theoretical perspectives to analyze the streaming data [33]. We consider the mobility of users under one PHA. Our model can be extended to design multilevel and distributed forms to make this more manageable and concurrently operable.

The main objective of this Information Technology (IT) based system is to make solutions feasible to computation, and that can control the further transmission of diseases. However, as in practical situations, we should also follow other pre-existing processes like social distancing, partial lockdown, preventive measures like washing hands, disinfection must continue for controlling infections.

ACKNOWLEDGMENT

GM acknowledges Post-graduate Division of Asutosh College, University of Calcutta for financial support and computational resources. PP acknowledges Bar-Ilan University for providing Kolam-Soref postdoctoral fellowship.

REFERENCES

- [1] R. Hinch et al., Effective configurations of a digital contact tracing App: A report to NHSX, 2020.
- [2] Singh, Rajesh and Adhikari, Ronojoy, Age-structured impact of social distancing on the COVID-19 epidemic in India, arXiv preprint arXiv:2003.12055, 2020.
- [3] Karin, Omer et al., Adaptive cyclic exit strategies from lockdown to suppress COVID-19 and allow economic activity, medRxiv, Cold Spring Harbor Laboratory Press, 2020.
- [4] Meidan, Dror and Cohen, Reuven and Haber, Simcha and Barzel, Baruch, An alternating lock-down strategy for sustainable mitigation of COVID-19, arXiv preprint arXiv:2004.01453, 2020.
- [5] Mark Zastrow, Coronavirus contact-tracing apps: can they slow the spread of COVID-19?, Nature, 2020.
- [6] Kelly Servick, COVID-19 contact tracing apps are coming to a phone near you. How will we know whether they work?, Science, 2020.
- [7] Hellewell, Joel et. al, Feasibility of controlling COVID-19 outbreaks by isolation of cases and contacts, The Lancet Global Health, Elsevier, 2020.

- [8] World Health Organization and others, Coronavirus disease 2019 (COVID-19): situation report, 107, World Health Organization, 2020.
- [9] De Carli, A and Franco, M and Gassmann, A and Killer, C and Rodrigues, B and Scheid, E and Schoenbaechler, D and Stiller, B, WeTrace—A Privacy-preserving Mobile COVID-19 Tracing Approach and Application, arXiv preprint arXiv:2004.08812, 2020.
- [10] Ferretti, Luca and Wymant, Chris and Kendall, Michelle and Zhao, Lele and Nurtay, Anel and Abeler-Dörner, Lucie and Parker, Michael and Bonsall, David and Fraser, Christophe, Quantifying SARS-CoV-2 transmission suggests epidemic control with digital contact tracing, *Science* 368 (6491), 2020.
- [11] Keeling, Matt J and Hollingsworth, T Deirdre and Read, Jonathan M, The Efficacy of Contact Tracing for the Containment of the 2019 Novel Coronavirus (COVID-19), medRxiv, Cold Spring Harbor Laboratory Press, 2020.
- [12] T. TraceTogether, How does TraceTogether work?, <https://tracetogogether.zendesk.com/hc/en-sg/articles/360043543473-How-does-TraceTogetherwork->, 2020, accessed: 2020-03-23.
- [13] , Covid Watch, url<https://www.covid-watch.org/>, accessed: 2020-05-11, 2020.
- [14] , Sydney Von Arx, Daniel Blank, Slowing the Spread of Infectious Diseases Using Crowdsourced Data, Covid Watch, 2020.
- [15] Rivest, R et. al, The PACT protocol specification, 2020.
- [16] Privacy-Preserving Contact Tracing, 2020. <https://www.apple.com/covid19/contacttracing>, accessed:2020-05-11
- [17] Government of India, Aarogya Setu Mobile App, 2020. <https://www.mygov.in/aarogya-setu-app/>, Accessed:09-05-2020
- [18] Oliver, Nuria et. al, Mobile phone data for informing public health actions across the COVID-19 pandemic life cycle, American Association for the Advancement of Science, 2020.
- [19] Hernández-Orallo, Enrique and Manzoni, Pietro and Calafate, Carlos T and Cano, Juan-Carlos, Evaluating how smartphone contact tracing technology can reduce the spread of infectious diseases: the case of COVID-19, *IEEE Access*, 2020.
- [20] Amit, Moran and Kimhi, Heli and Bader, Tarif and Chen, Jacob and Glassberg, Elon and Benov, Avi, Mass-surveillance technologies to fight coronavirus spread: the case of Israel, *Nature Medicine*, 2020.
- [21] Maxmen, Amy, Can tracking people through phone-call data improve lives?, *Nature*, 569(7758), 2019.
- [22] Ben Lovejoy, Turing algorithms may improve accuracy of Apple/Google contact tracing API, 2020. <https://9to5mac.com/2020/06/29/turing-algorithms/>, accessed:2020-06-29
- [23] Allen, Danielle, Securing Justice, Health, and Democracy against the COVID-19 Threat, 2020.
- [24] Moneycontrol News, WHO warning on COVID-19: 'Not even close to being over. Worst is yet to come', 2020. <https://www.moneycontrol.com/news/trends/health-trends/coronavirus-pandemic-worst-is-yet-to-come-who-wars-5480611.html>, accessed:2020-
- [25] Bar-On, Yinon M and Flamholz, Avi and Phillips, Rob and Milo, Ron, Science Forum: SARS-CoV-2 (COVID-19) by the numbers, *eLife* 9, e57309 2020.
- [26] Cormen, Thomas H and Leiserson, Charles E and Rivest, Ronald L and Stein, Clifford, Introduction to algorithms, 2009, MIT press.
- [27] Silberschatz, Abraham and Korth, Henry F and Sudarshan, Shashank, Database system concepts, McGraw-Hill New York, 1997.
- [28] Zhong, Xin, Bluetooth Low Energy Application in home automation, 2019.
- [29] Garcia-Molina, Hector and Ullman, Jeffrey D and Widom, Jennifer, Database system implementation, Prentice Hall Upper Saddle River, NJ, 2000.
- [30] Danon, Leon and Read, Jonathan M and House, Thomas A and Vernon, Matthew C and Keeling, Matt J, Social encounter networks: characterizing Great Britain, *Proceedings of the Royal Society B: Biological Sciences*, 280(1765), 2013.
- [31] Bengio, Yoshua et. al, The need for privacy with public digital contact tracing during the COVID-19 pandemic, *The Lancet Digital Health*, Elsevier, 2020.
- [32] Mello, Michelle M and Wang, C Jason, Ethics and governance for digital disease surveillance, *Science* 368(6494), 951-954, 2020.
- [33] McGregor, Andrew, Graph stream algorithms: a survey, *ACM SIGMOD Record* 43(1), 9-20, ACM New York, NY, USA, 2014.

Appendix: Dynamic Graph Streaming Algorithm for Digital Contact Tracing

Gautam Mahapatra^{1,2}, Priodyuti Pradhan³, Ranjan Chattaraj², and Soumya Banerjee⁴

1. Computer Science, Asutosh College, University of Calcutta, Kolkata, West Bengal, India
2. Computer Science and Engineering, Birla Institute of Technology, Mesra, Off-Campus Deoghar, Jharkhand, India
3. Complex Network Dynamics, Department of Mathematics, Bar-Ilan University, Ramat-Gan, Israel
4. Inria EVA, Paris, France & Director Innovation Smart City EU.

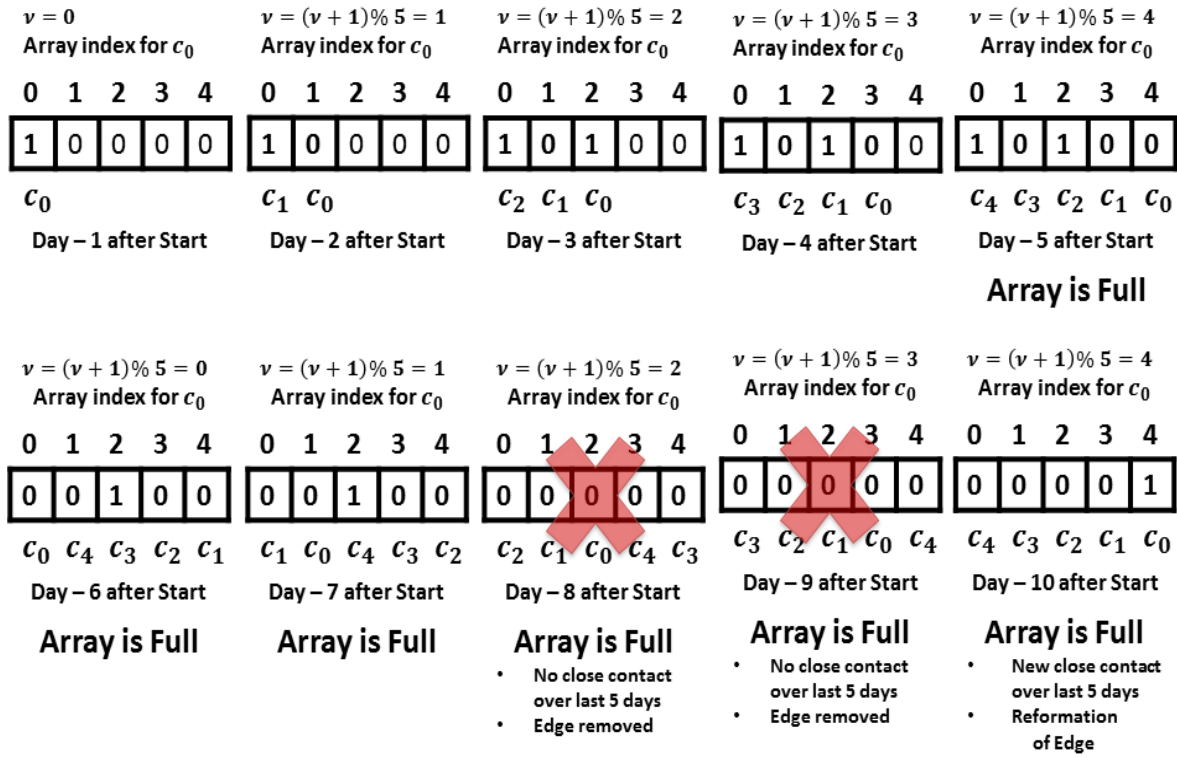


Fig. A1. Illustration of the array-based circular queue implementation using modular-arithmetic for sliding window of the contact vector $c_{(P, P')}$ in \mathcal{G} . For simplicity, we consider $D = 5$ days, $\tau = 1$ day, so size of the contact vector is $n = 5$. After D days $c_{(P, P')}$ attends the full length. Here, $c = 0$ means there is no close contact during the latest D days, so the possibility of infection transmission is nullified, and hence respective edge will be removed. However, they may come in close contact again. A new contact vector will be formed after synchronization with system deployment time.